JOURNAL OF MATERIALS SCIENCE 31 (1996) 6105–6111

The effect of hydrogen on the strength and superplastic deformation of beta-titanium alloys

HAO ZHANG
Department of Materials Science and Engineering, University of Cincinnati, Cincinnati, OH 45221, USA

TIM FAI LAM
Advanced Micro Devices (Singapore) PTE Ltd, Singapore 1646

JIALONG XU
Shanghai Iron and Steel Research Institute, Shanghai 200940, People's Republic of China

SHIHONG WANG
Department of Materials Science and Engineering, Beijing University of Aeronautics and Astronautics, Beijing 100083, People's Republic of China

The effect of hydrogen on mechanical properties and superplastic deformation of two commercial β titanium alloys, Ti–4Al–7Mo–10V–2Fe–1Zr (Ti–471021) and Ti–10V–2Fe–3Al (Ti–1023), was studied in the range of hydrogen concentration up to 1.3 wt%. The elevated temperature hardness of Ti–471021 alloy increased with hydrogen concentration. The stress levels during the superplastic deformation in both alloys increased with increasing concentrations of hydrogen in the β-phase region. X-ray diffraction results and examination of the microstructure with TEM revealed that no hydrides had formed up to hydrogen concentrations of 1.3 wt%. The increase in flow stress was mainly due to the solid solution strengthening by hydrogen during the superplastic deformation.

1. Introduction

Hydrogen has long been considered to have detrimental effects on mechanical properties of titanium alloys [1–3]. However, it has also been demonstrated that hydrogen has beneficial effects in improving hot workability, refining microstructure, and enhancing mechanical properties of titanium alloys [4–11]. Kolachev *et al.* reported that the addition of hydrogen caused a remarkable decrease in forging loads and improved the hot workability in Ti–9Al [4] and Ti–5Zr–9Al–5Sn–2Mo [5] alloys. Birla and DePierre [6] reported that the forging flow stress of Ti–6Al–2Sn–4Zr–6Mo alloy decreased by 30%–35% at 730 °C with the addition of 0.4 wt % hydrogen. Kerr *et al.* [7] studied the effects of hydrogen on the hot workability of Ti–6V–4Al by using hydrogen as a temporary alloying element. They reported that hydrogen stabilized the β-phase and reduced the forging flow stress by 30%. This reduction was equivalent to decreasing the forging temperature by 80 °C. Their results showed a minimum flow stress was obtained at a hydrogen concentration of 0.2–0.4 wt %. Kerr *et al.* suggested that hydrogen, as a potent β stabilizer, suppressed the β transus temperature and increased the volume ratio of β/α in Ti–6Al–4V alloy for a given testing temperature. Because bcc β-phase possessed much better hot workability than α-phase, the introduction of a certain amount of hydrogen improved the hot workability in α and α + β alloys. They also reported that when the hydrogen concentration was more than 0.4 wt %, the flow stress increased due to the formation of hydrides in the microstructure [7]. Hydrogen also improved the superplasticity in titanium alloys such as Ti–6Al–4V [10, 11]. Zhang *et al.* [11] reported the optimum range of hydrogen concentration for superplasticity of Ti–6Al–4V alloy was approximately 0.2–0.3 wt %. This was attributed to an optimization of the β/α ratio in the α + β alloy. At higher hydrogen concentrations, the hydrogen caused the formation of hydrides and a fully stabilized β microstructure. This resulted in rapid grain growth and reduced superplasticity in Ti–6Al–4V alloy [10, 11].

While the effects of hydrogen on α and α + β alloys at elevated temperatures have been well documented, few studies have been reported on the effects of hydrogen on β alloys, particularly at elevated temperatures [12]. Because there is a great difference in properties between α + β alloys and β alloys, differences in the hydrogen effects on both are expected. The major issues relevant to the different effects of hydrogen between β and α + β titanium alloys result from the difference in hydrogen solubility. Hydrogen has a solubility which is much higher in β alloys than in

0022–2461

α and α + β alloys [13, 14]. In the β-annealed condition, hydrogen solubility in the β-titanium alloys are as high as more than 1 wt % in some alloy systems [1, 12, 14–16]. In addition, hydrogen has a diffusivity approximately ten times higher in β-phase than in α-phase [14].

The objectives of the present work were to investigate the effects of hydrogen on the mechanical properties of β-titanium alloys at elevated temperatures, and compare the hydrogen effects on the mechanical properties of β alloys at room and elevated temperatures. In carrying out this work, superplastic tensile tests were conducted in two commercial β-titanium alloys, Ti–4Al–7Mo–10V–2Fe–1Zr (Ti–471021) and Ti–10V–2Fe–3V (Ti–1023), in the single β-phase region. This eliminated the indirect effects from other phases such as α, ω and hydride.

2. Experimental procedure

The materials used in this study were two commercial β-titanium alloys, Ti–4Al–7Mo–10V–2Fe–1Zr (Ti–471021) and Ti–10V–2Fe–3Al (Ti–1023), supplied as hot-rolled bars with the diameter of 25 mm. The chemical composition of these two alloys is listed in Table I. The bars were further hot-rolled to reduce the diameter to 19 mm, then annealed at 800 °C for 30 min in an argon atmosphere and water quenched. Tensile specimens and other specimens were machined from the bars. The tensile specimens were 5 mm diameter and 20 mm gauge length.

The previously machined specimens were charged with hydrogen to various concentrations in a Sieverts apparatus in a sealed chamber at 800 °C for 3 h. The introduced hydrogen was controlled by the hydrogen partial pressure in a mixed gas of hydrogen and argon in accordance with Sievert's law: $C_H = K(P_{H_2})^{1/2}$. C_H is the hydrogen concentration in the specimen, P_{H_2} is the partial pressure of the hydrogen, and K is a constant. Specimens were water quenched after being charged with hydrogen. Hydrogen concentrations in the specimens were determined by measuring the weight of the specimens before and after the hydrogen charging with a 0.000 01 g balance. Chemical analysis was also used to confirm the hydrogen concentrations in some specimens. The results indicated a very good agreement between these two methods.

Standard metallographic procedures were used to prepare the specimens for optical metallography and X-ray diffraction tests. Metallographic specimens were etched with Kroll's etchant. X-ray diffraction measurements were conducted with a Siemens D-500 diffractometer using CuK_α radiation. The strain rate for the room-temperature tensile test was $4.5 \times 10^{-4}\ s^{-1}$. Elevated temperature hardness tests were conducted in a special chamber maintaining the proper H_2/Ar gas ratio for a given hydrogen concentration. Superplastic tensile tests were performed on a universal testing instrument at 800 °C. The tensile specimens were placed in a sealed, heated, environmental chamber. Hydrogen concentrations in the test samples were maintained during heating and testing by flowing a gas mixture of hydrogen and argon through the chamber. The H_2/Ar ratio was selected based on the desired hydrogen concentration. During the superplastic tests the crosshead rate was held constant at $0.5\ mm\ min^{-1}$ (initial strain rate $\dot{\varepsilon}_0 = 4.5 \times 10^{-4}\ s^{-1}$). Load–elongation curves and true stress–true strain curves were recorded. The fractured specimens were sectioned longitudinally from the grips (undeformed) through the gauge lengths (deformed) for further studies by optical microscopy and transmission electron microscopy (TEM). The TEM thin foil preparation was by electro-chemical double jet polishing. The electrolytic solution used was 6% perchloric acid ($HClO_4$) + 34% *n*-butyl alcohol + 60% methanol employing a voltage of 40 V and at a temperature of − 40 °C.

3. Results

3.1. Microstructure and X-ray diffraction

Optical micrographs of these two β-treated alloys containing different hydrogen concentrations are shown in Fig. 1. The optical microstructure was all β-phase with the grain sizes approximately 100 μm for Ti–471021 and 80 μm for Ti–1023. The grain size was found to be independent of hydrogen concentration. Up to 1.3 wt % hydrogen, no hydrides were found by examination with X-ray diffraction and TEM in all specimens of both alloys. This was in agreement with the previous studies on the hydrogen solubility of β-phase in β-titanium alloys [14–18].

The variation in the lattice constants of the β-phase in both alloys with hydrogen concentration was measured by X-ray diffraction at room temperature and is shown in Fig. 2. The lattice constant of Ti–471021 expanded by 1.0% at the hydrogen concentration of 1.1 wt %. For Ti–1023, the lattice constant increased 1.4% as the hydrogen concentration increased to 1.3 wt %. These results agree with those reported by Paton *et al.* for Ti–18 wt % Mo [17] and by Young and Scully for Ti–Al–Nb–Mo [19].

3.2. Room-temperature tensile test

The effects of hydrogen on room-temperature tensile properties of Ti–471021 are shown in Fig. 3. The tensile yield strength initially increased slightly with hydrogen concentration and then decreased. The ductility of the alloy initially decreased slightly and then decreased rapidly beginning at a nominal hydrogen

TABLE I Chemical composition of Ti–4Al–7Mo–10V–2Fe–1Zr and Ti–10V–2Fe–3Al alloys used in this study (wt %)

Alloys	Ti	Al	Mo	V	Fe	Zr	Si	C	H	O
Ti–471021	Bal.	4.05	7.24	9.64	1.85	0.89	0.05	0.02	0.0062	0.016
Ti–1023	Bal.	3.08	–	9.46	1.98	–	0.02	0.03	0.0023	0.085

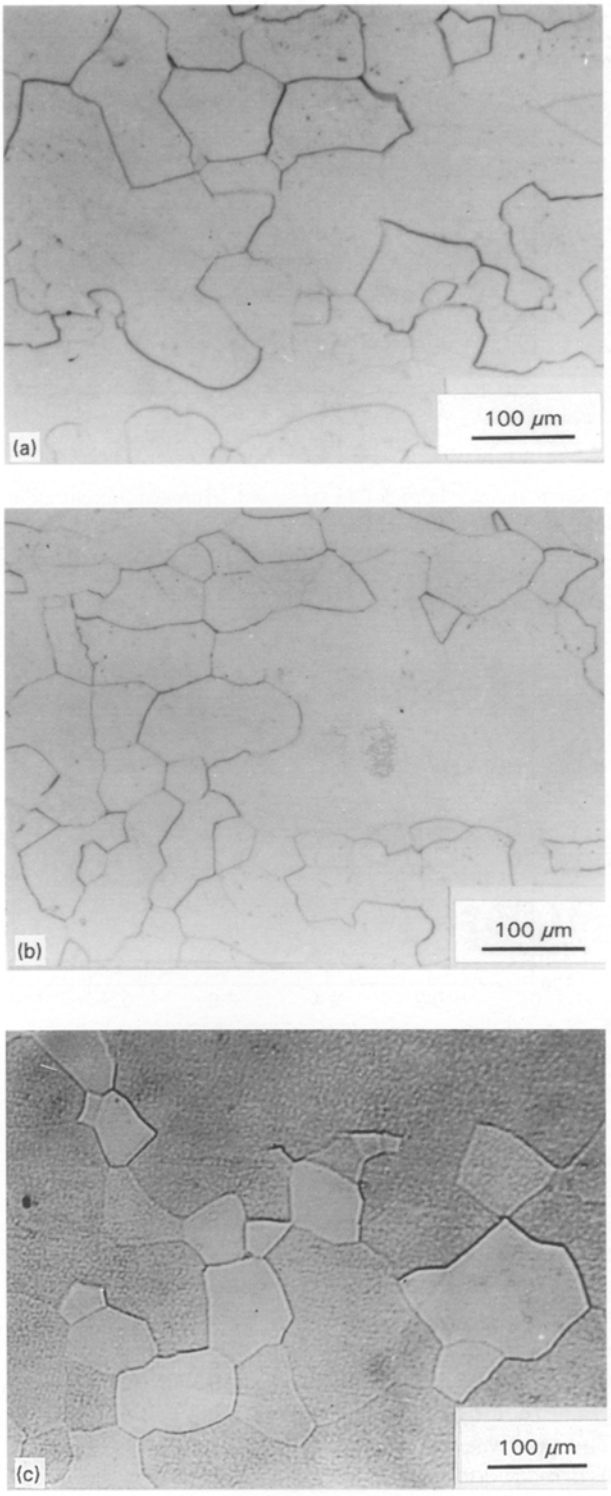

Figure 1 Optical micrographs of two β-titanium alloys containing different hydrogen concentrations: (a) Ti–471021 containing H = 0.0062 wt %, (b) Ti–471021 containing H = 1.15 wt %, (c) Ti–1023 containing H = 0.0023 wt %.

concentration of 0.25 wt %. The initial increase in yield stress might indicate hydrogen strengthening in this alloy. At higher hydrogen concentrations, the alloy was so brittle that the specimens fractured before any apparently plastic deformation took place. The arrow line in Fig. 3 shows the trend of the decrease in the yield stress with increasing hydrogen concentration.

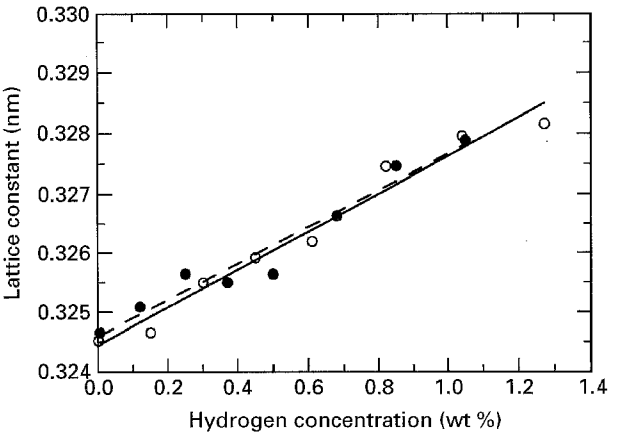

Figure 2 Variation of lattice constants with hydrogen concentrations for (--●--) Ti–471021 and (—○—) Ti–1023 alloys.

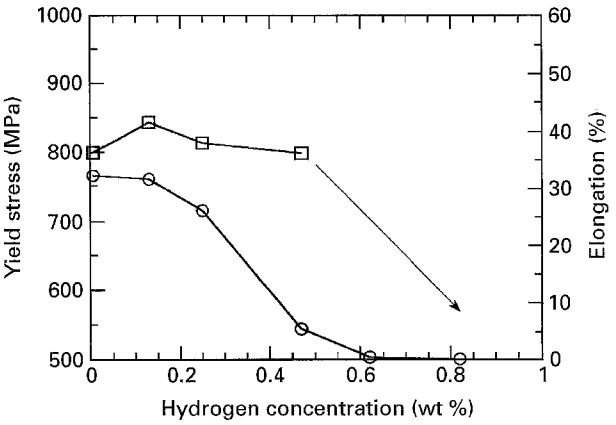

Figure 3 Effect of hydrogen on room-temperature tensile properties of Ti–471021: (□) yield stress, (○) elongation.

3.3. Hardness at elevated temperatures

The variations in hardness of Ti–471021 with hydrogen concentration at elevated temperatures are shown in Fig. 4. Note the hardness increased with hydrogen at all testing temperatures, indicating the solid-solution strengthening by hydrogen in β-titanium at elevated temperatures.

3.4. Effect of hydrogen on superplastic deformation

The true stress–true strain curves for the superplastic deformation of Ti–471021 and Ti–1023 alloys containing different hydrogen concentrations are shown in Fig. 5. Both alloys showed similar superplastic behaviour and the same hydrogen effects. The entire stress level of the superplastic deformation increased with hydrogen concentration, indicating the strengthening by hydrogen in β alloys at elevated temperature. The increase in peak flow stress and the variations of elongation of the two alloys with hydrogen concentration are shown in Figs 6 and 7, respectively. The elongation of both alloys slightly decreased initially then increased for higher hydrogen concentrations. The strain rate sensitivity, m, of the specimens containing base hydrogen concentrations were 0.38 and 0.54 for Ti–471021 and Ti–1023 during the superplastic deformation, respectively.

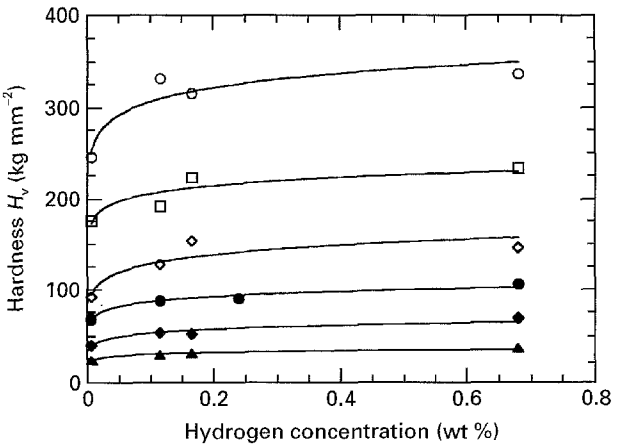

Figure 4 Variation of Vickers' hardness with temperature and hydrogen concentration for Ti–471021 (load 5 kg): (○) 500 °C, (□) 600 °C, (◇) 650 °C, (●) 700 °C, (◆) 750 °C, (▲) 800 °C.

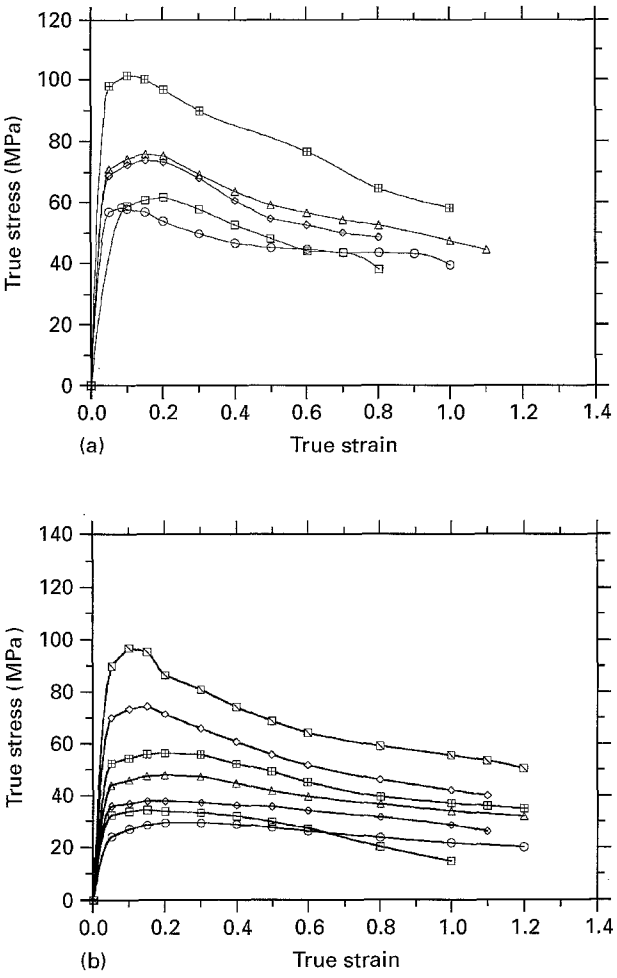

Figure 5 True stress–true strain curves of superplastic deformation for both β-titanium alloys containing different hydrogen concentrations at 800 °C: (a) Ti–471021, (b) Ti–1023. Hydrogen concentrations (wt %): (a) (○) 0.0062, (□) 0.17, (◇) 0.21, (△) 0.40, (⊞) 0.56; (b) (○) 0.0023, (□) 0.31, (◈) 0.35, (△) 0.52, (⊞) 0.78, (◇) 0.82, (◰) 0.95.

3.5. Microstructure after superplastic deformation

Fig. 8a and b show the optical microstructure of Ti–471021 after superplastic deformation at 800 °C. Before the test, grains had the characteristic equiaxed appearance of β-annealed alloys. Significant changes

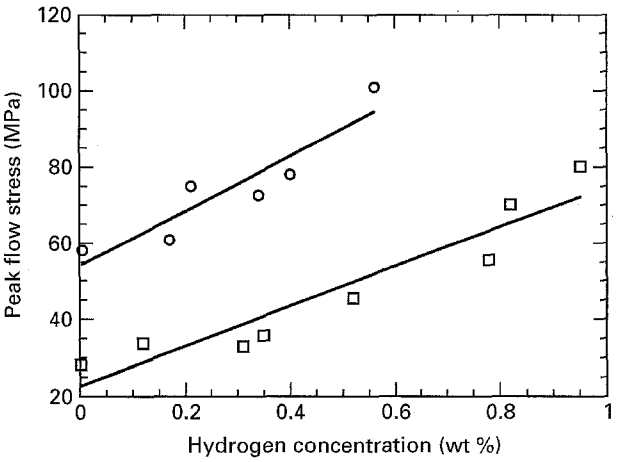

Figure 6 Increase in peak flow stress with hydrogen concentration for (—○—) Ti–471021, and (—□—) Ti–1023.

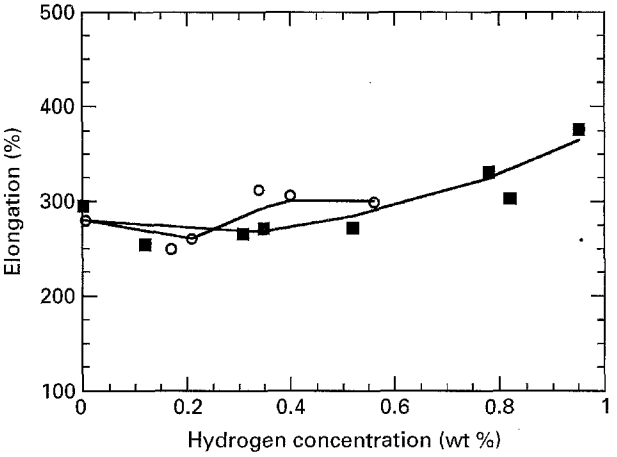

Figure 7 Variations of superplastic elongation with hydrogen concentration for (—○—) Ti–471021, and (—■—) Ti–1023.

occurred and the β grains became much finer after the superplastic deformation. The main change in the microstructure was the formation of large amounts of subgrains in the β-phase. The measurement of grain size, which is given in Fig. 9, revealed that the β grain size of the deformed microstructure slightly decreased with hydrogen. This suggests that hydrogen causes grain refining during the superplastic deformation. The decrease in grain size with hydrogen at high hydrogen concentrations correlated with a slight increase in the elongation of the alloys during superplasticity as mentioned earlier. The microstructure and substructure of both alloys were also observed using TEM. Fig. 10 shows a transmission election micrograph of the subgrain structure in a superplastically deformed Ti–471021 specimen containing 0.82 wt % hydrogen. The transmission electron micrograph in Fig. 11 of Ti–471021 containing 0.0062 wt % hydrogen shows dislocations after superplastic deformation. Evidence of hydrides or α-phase could not be found in any specimen of either alloy. This indicates the increase in flow stress resulted from the strengthening effect of hydrogen, rather than the strengthening due to other phases.

Previous work [20, 21] has reported that β-titanium alloys with large grain size exhibit superplasticity

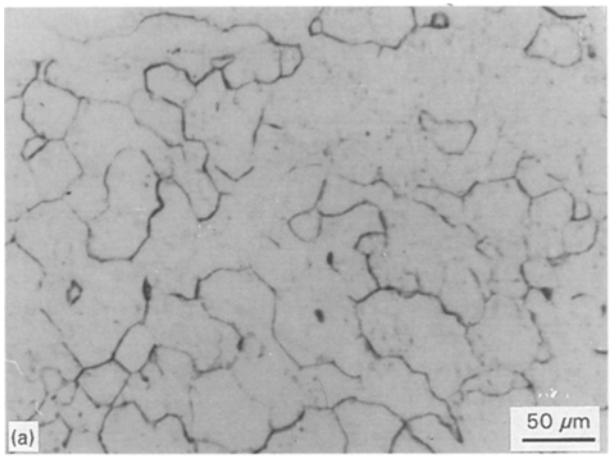

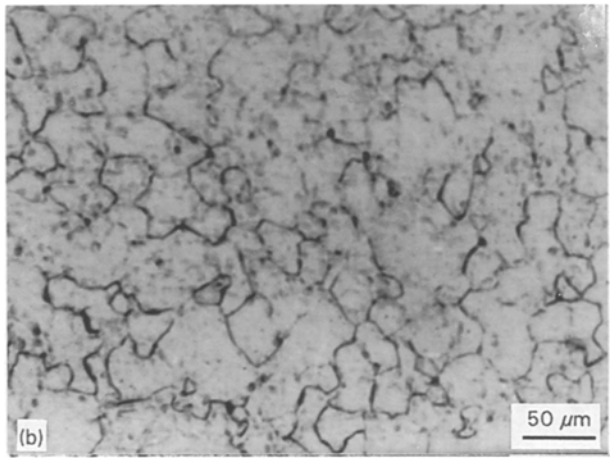

Figure 8 Optical micrographs of longitudinal sections from the deformed gauge of a Ti–471021 sample after superplastic deformation, showing development of subgrain structure: (a) H = 0.21 wt %, (b) H = 0.56 wt %. The testing temperature was 800 °C

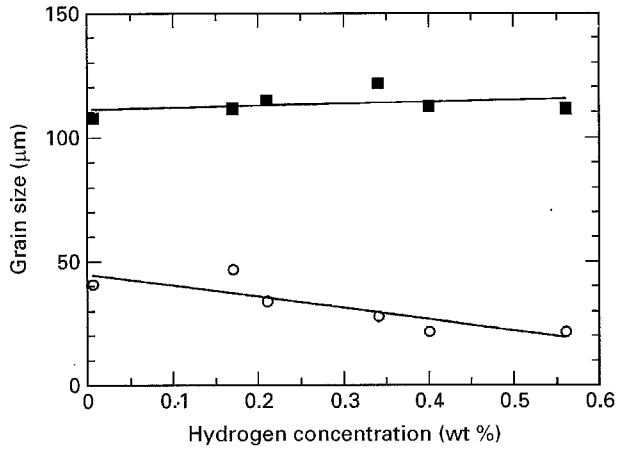

Figure 9 β-phase grain size of Ti–471021 as the function of hydrogen concentration after superplastic deformation at 800 °C: (○) deformed region, (■) undeformed region.

under certain conditions. Different superplastic deformation mechanisms were proposed for large-grained β alloys (with the grain size of 100 μm) compared to the mechanisms proposed for α + β alloys with the grain size range of 5–10 μm. Hammond and co-workers [20, 21] reported that subgrain structure was formed at an early stage during superplastic deformation in the β-phase region, and remained as the deformation proceeded. The formation and migration of subgrain boundaries, which was probably controlled by dislocation generation and climb mechanisms, maintained an equiaxed grain structure during the superplastic deformation in the β-phase region [20, 21]. In this work, the examination of microstructure revealed similar microstructural characteristics in the superplastically deformed Ti–471021 and Ti–1023 with and without hydrogen.

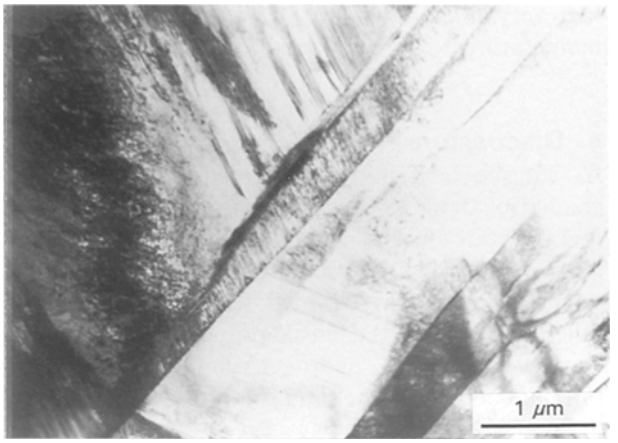

Figure 10 Transmission electron micrograph of Ti–1023 containing 0.82 wt % hydrogen after deformation at 800 °C. This shows the sub-grain boundary networks formed during superplastic deformation.

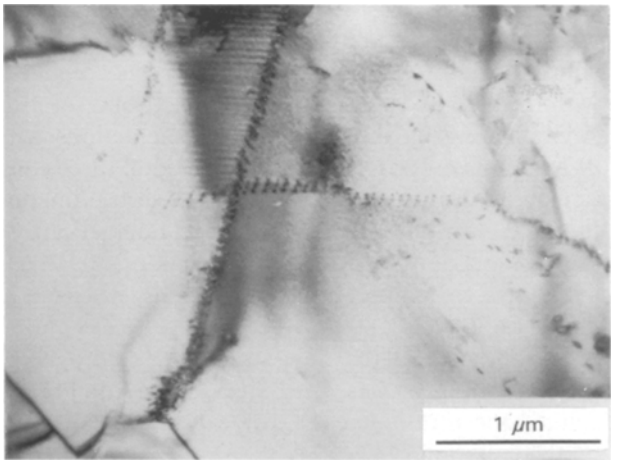

Figure 11 Transmission electron micrograph of Ti–471021 containing 0.0062 wt % hydrogen after superplastic deformation at 800 °C, showing dislocation configuration.

Hydrogen was either in interstitial solid solution or trapped at various defects such as dislocations, grain boundaries and inclusions in titanium alloys. The presence of hydrogen caused strengthening of the alloys due to the interaction between hydrogen and dislocations. In addition, the interaction between hydrogen and grain boundaries inhibited grain-boundary slip and grain migration. The solution strengthening effect was responsible for both the net increase in each flow stress curve and the increase in peak stress with increasing hydrogen concentration. For each curve the high level was largely retained during deformation due to the fact that the hydrogen

had very high diffusivity in β-titanium at elevated temperatures.

4. Discussion

As can be seen in Fig. 3, hydrogen effected little change in strength but seriously impaired the ductility of Ti–471021 alloy at room temperature. Comparison of the variation in the strength with hydrogen at room temperature and at elevated temperature indicated different effects on the tensile properties of β alloy. At room temperature, hydrogen embrittlement of β-titanium occurred. The solid solution strengthening of hydrogen was not as strong as at elevated temperature because the alloys were so embrittled that the specimens fractured before the apparently plastic deformation. This occurred both at medium and high hydrogen concentrations. Therefore, the interaction between hydrogen and dislocations did not take place to a significant extent. At elevated temperature, the elongations for fracture of both alloys initially decreased slightly and then increased with hydrogen concentration to surpass the levels for the specimens with the base hydrogen concentrations. Solid solution strengthening by interstitial atom interactions with dislocations in the alloys are comprised of three components [22]: the elastic interaction, electric interaction and chemical interaction (Suzuki interaction). Of these interactions, the electric interaction is relatively insensitive to temperature and remains, in effect, at about 0.6 T_m [23].

The increase in the flow stress with hydrogen in β-titanium alloys was attributed to the equilibrium solute concentration near a dislocation which is given by the equation [24]

$$C = C_0 \exp(U/kT) \quad (1)$$

where C_0 is the average concentration and U is the interaction energy between solute and dislocation. At a given temperature, C increases with C_0. Therefore, the increase in C causes flow stress increase during the deformation process. The equation also indicates that for a given solute, the magnitude of the interaction of solute and dislocation increases with increasing solute concentration [24].

As shown in Fig. 5b, the presence of hydrogen resulted in the appearance of a flow peak in the tests of Ti–1023 containing different hydrogen concentrations. The flow peak did not appear in the control sample containing the base hydrogen concentration. In Ti–471021, the flow peak was enhanced by hydrogen. In the present study, the increase of peak flow stress was due to the interaction between hydrogen atoms and dislocations. Vijayshankar and Ankem [25] have reported a flow stress peak and a following abrupt drop off in high-temperature tensile deformation behaviour of Ti–Mn and Ti–V alloys. Their results indicated some types of dislocations–solute atoms interaction in binary titanium alloys.

Costa *et al.* [14, 15] classified the effects of hydrogen on titanium alloys into two categories, i.e. "intrinsic" effects and "indirect" effects. The "intrinsic" effects of hydrogen were independent of microstructural modification, and directly influenced the lattice of β-titanium, while the "indirect" effects were attributed to the changes in microstructure and phases due to the presence of hydrogen in titanium alloys. At room temperature, metastable β-titanium alloys usually consist of other phases beside β, such as α, α″ and ω in Ti–1023, and α and ω in Ti–471021 after solid solution treatment in the β region and water quenching. Changes in the relative amounts of these phases caused variations in the mechanical properties of the alloys. Previous studies have reported the "indirect" effects of hydrogen due to its influence on microstructural modifications of α, α″ and ω phases in Ti–1023 [15], α and ω phases in Ti–20V [18]. It is difficult to separate the "intrinsic" and "indirect" effects of hydrogen on the tensile properties of β alloys after solid solution treatment in the β region and water quenching, because the specific effect of hydrogen on the tensile property of a particular alloy also depends on the stability of β and other phases in the alloys [14]. Because the "indirect" effects from other phases such as α, ω and hydride were eliminated at elevated temperatures, the tensile tests at elevated temperatures demonstrated the "intrinsic" effect of hydrogen on β-titanium alloys.

There was no significant solid solution strengthening by hydrogen at high concentrations reported in β-titanium alloys due to the significant loss in ductility of the alloys as the hydrogen was increased. At high hydrogen concentrations, the alloys were so brittle that the specimens readily fractured before any perceptible macro-deformation occurred at room temperature. Therefore, the interaction of hydrogen and dislocations did not take place to a significant extent. In the present study, the superplastic tensile tests at elevated temperature illustrated the extensive interaction between hydrogen and dislocations during the entire deformation process.

5. Conclusions

The effect of hydrogen on mechanical properties and superplastic deformation of two commercial β-titanium alloys, Ti–4Al–7Mo–10V–2Fe–1Zr (Ti–471021) and Ti–10V–2Fe–3Al (Ti–1023), was studied for hydrogen concentrations up to 1.3 wt %. The elevated temperature hardness of Ti–471021 alloy increased with hydrogen concentration. The entire stress levels of the superplastic deformation in both alloys increased with increasing levels of hydrogen in β phase region. X-ray diffraction and TEM results revealed that no evidence of hydrides had been formed up to hydrogen concentrations of 1.3 wt %. The increase in flow stress was mainly due to solid solution strengthening by hydrogen, which resulted from the interaction between hydrogen and dislocations during superplastic deformation.

Acknowledgement

The support received from Shanghai Iron and Steel Research Institute is gratefully acknowledged.

References

1. N. E. PATON and J. C. WILLIAMS, "Hydrogen in Metals", edited by I. M. Bernstein and A. W. Thompson (ASM, OH, 1974) pp. 409–32.
2. G. A. LENNING, C. M. GRAIGHEAD and R. I. JAFFEE, *Trans. AIME* **200** (1954) 367.
3. D. N. WILLIAMS, *J. Inst. Metals* **91** (1962–1963) 147.
4. B. A. KOLACHEV, V. K. NOSOV, V. A. LIVANOV, G. I. SHCHIPUNOV and A. D. CHUCHUNUKIN, *Izv. Vyssh. Uchekn. Zaved. Tsvetn. Metall.* (4) (1972) 137 (USAF Foreign Technology Division Translation, FTD-ID(RS) 1-1076-76, August 1976).
5. B. A. KOLACHEV, V. K. NOSOV, V. A. LIVANOV, G. I. SHCHIPUNOV and S. M. FAYNBRON, *Kuzechn Shtampov. Proizv.* (1) (1975) 29 (USAF Foreign Technology Division Translation, FTD-ID(RS) 1-1347-75, November 1975).
6. N. BIRLA and V. DePIERRE, Technical Report AFML-TR-75-171, US Air Force materials Laboratory, Wright-Patterson Air Force Base, OH, October 1975.
7. W. R. KERR, P. R. SMITH, L. R. BIDWELL, M. E. ROSENBLUM, F. J. GURNEY and Y. MAHAJAN, in "Titanium'80 Science and Technology" (Conference Proceedings) edited by H. Kimura and O. Izumi (TMS-AIME, Warrendale, PA, 1980) pp. 2477–86.
8. W. R. KERR, *Metall. Trans.* **16A** (1985) 1077.
9. F. H. FROES and D. EYLON, in "Hydrogen Effects in Materials Behavior", edited by N. R. Moody and A. W. Thompson (TMS, Warrendale, PA, 1990) pp. 261–82.
10. R. J. LEDERICH, S. M. L. SASTRY, J. E. O'NEAL and W. R. KERR, in "Advanced Processing Methods for Titanium", edited by D. E. Hasson and C. H. Hamilton (TMS-AIME, Warrendale, PA, 1982) pp. 115–28.
11. H. ZHANG, J-L. XU, T-H. LIN, W-D. WENG, P-L. MAO and S-H. WANG, *Rare Metal Mater. Eng.* **20** (1991) 52.
12. HAO ZHANG, TIENHUI LI, JIALONG XU, SHIHONG WANG, in "Superplasticity and Superplastic Forming", edited by A. K. Ghosh and T. R. Bieler (TMS, Warrendale, PA, 1995) pp. 109–16.
13. M. HANSEN, "Constitution of Binary alloys" (McGraw-Hill, New York, 1958).
14. J. E. COSTA, D. BANERJEE and J. C. WILLIAMS, in "BetaTitanium Alloys in the 1980s", edited by R. Boyer and H. W. Rosenberg (TMS-AIME, Warrendale, PA, 1983) pp. 69–84.
15. J. E. COSTA, J. C. WILLIAMS and A. W. THOMPSON, *Metall. Trans.* **18A** (1987) 1421.
16. T-H. LIN, H. ZHANG W-D. WENG, N-Y. PAN and C-M. HSIAO, *Scripta Metall.* **23** (1989) 891.
17. N. E. PATON and O. BUCK, in "Effect of hydrogen on Behavior of Materials", edited by A. W. Thompson and I. M. Bernstein (AIME, New York, 1976) pp. 83–90.
18. N. E. PATON, R. SPURLING and C. G. RHODES, "Hydrogen Effect in Metals" (TMS-AIME, Warrendale, PA, 1981) pp. 260–79.
19. G. A. YOUNG Jr and J. R. SCULLY, *Scripta Metall. Mater.* **28** (1993) 507.
20. P. GRIFFITHS and C. HAMMOND, *Acta Metall.* **20** (1972) 935.
21. G. C. MORGAN and C. HOMMOND, *Mater. Sci. Eng.* **86** (1987) 159.
22. R. L. FLEISCHER, in "The Strengthening of Metals", edited by D. Pechner (Reinhold Publishing Corp., New York, 1967) p. 93.
23. G. E. DIETER, "Mechanical Metallurgy", 3th Edn (McGraw-Hill, New York, 1986) p. 205.
24. E. O. HALL, "Yield Point Phenomenon in Metals and Alloys" (Plenum, New York, 1985).
25. M. N. VIJAYSHANKAR and S. ANKEM, *Mater. Sci. Eng.* **A129** (1990) 229.

Received 6 February 1995
and accepted 13 February 1996